Influence of an oblique magnetic field on planar flame front instability

Mako Sato and Yasuhide Fukumoto

Abstract We investigate the effect of external magnetic field on the Darrieus-Landau instability (DLI), the linear instability of a planar premixed flame front, in an electrically conducting fluid. This setting has applicability to combustion phenomena of the astrophysical scale. Without magnetic field, the planar flame front is necessarily unstable. Previous investigation treated independently the normal and tangential magnetic fields. Here we focus on the case of their simultaneous application, namely, oblique magnetic field. Rederiving the jump conditions, across the flame front, of the physical variables based on the ideal magnetohydrodyamics equations, we correct the previous treatment of the Markstein effect and extend it to incorporate the disparity of the magnetic permeability. A genuinely oblique magnetic field has an unusual characteristics that discontinuity in tangential velocity across the flame is induced. It is found that the Kelvin-Helmholtz instability takes over the stabilizing effect on the DLI in a limited parameter regime when the normal Alfvén speed exceeds the normal fluid velocity in both the unburned and burned regions.

1 introduction

Combustion is a multiscale phenomenon of a reacting fluid from the molecular scale, on which a succession of complicated chemical reactions occur, to the hydrodynamic scale, flows of a fuel (= an unburned gas) and a burned gas on the

Mako Sato
Graduate School of Science, Osaka City University,
3-3-138 Sugimoto, Sumiyoshi-ku, Osaka 558-8585, Japan
e-mail: m20sa020@tx.osaka-cu.ac.jp

Yasuhide Fukumoto
Institute of Mathematics for Industry, Kyushu University,
744 Motooka, Nishi-ku, Fukuoka 819-0395, Japan
e-mail: yasuhide@imi.kyushu-u.ac.jp

macroscopic scale, as exemplified by the Bunsen burner and rocket engines [5]. It is a phenomenon whose precise description needs consideration of a number of chemical processes and the mixture and diffusion of a number of reactant species and the heat as well. If we consider combustion phenomena in the universe, such as explosion of supernovae, we have to include the magnetic field [9] which is macroscopically described by the Maxwell equations.

It may well be thought that we have to deal with an innumerable number of equations of governing an innumerable number of chemical species, hydrodynamic, thermodynamic variables and electro-magnetic fields. Extensive studies since the middle of the 20th centuries have clarified that the macroscopic scale behavior of a phenomena is somewhat independent from the microscopic processes, now being known as the concept of the scale separation. In this paper, we consider the combustion subjected to imposed magnetic field, on the hydrodynamic scale, of an electrically conducting fluid. We make the linear stability analysis of a planar front, of infinitesimal thickness, of a premixed flame, based on the equations of the ideal magnetohydrodynamics (MHD), consisting of the continuity and the Euler equations augmented by the induction equation for the magnetic field [10].

The Darrieus-Landau instability (DLI) is an exponential amplification, in time, of wavy deformations of a planar flame front of incompressible fluids (=burned and unburned gases), put forward independently by Darrieus (1938) and Landau (1944) [6, 13, 14]. For this treatment of the hydrodynamic instability, the flame front is reckoned as an infinitely thin interface with density discontinuity across it. In accordance, we skip chemical reactions occurring in it. Darrieus and Landau assumed that the flame front advances to the unburned gas (fuel) at a constant speed S_L, and dealt with the Euler equation and the continuity equation for an incompressible fluid. The growth rate n of the DLI is given by

$$\frac{n}{kS_L} = \frac{\alpha}{1+\alpha}\left(\sqrt{1+\alpha-\frac{1}{\alpha}}-1\right),$$

where $\alpha = \rho_u/\rho_b(>1)$, with $\rho_u(\rho_b)$ being the density of unburned (burned) gas, represents the thermal expansion and k is the wavenumber. The result of $n>0$ for all $\alpha(>1)$ means that a planer flame front is necessarily linearly unstable, with the growth rate being proportional to the wavenumber. However stable flame fronts are observed in experiments, which motivated successors to improve the original DLI. Markstein [15] considered effect of the flame front curvature on the flame speed S_f [5]. Matalon and Matkowsky [16] elaborated the Markstein effect based on the heat-conduction equation for the temperature and the diffusion equation for the reactant, and formulated the Markstein effect as the jump conditions, on the hydrodynamic scale, of the hydrodynamic and thermodynamic variables across the flame front. Class *et al.* [3, 4] devised the jump conditions to take account of chemical reactions through the heat release at the interface concomitant with the gas expansion.

For combustion phenomena in the universe, we have to add the induction equation *etc.* to the governing equations for plasmas, because the space around large-scale objects is filled with magnetic field. The magnetic field is expected to sup-

press the instability of an interface, and its influence has extensively studied for the Kelvin-Helmholtz (KHI), the Rayleigh-Taylor and the Richtmeyer-Meshkov instabilities [10, 17], toward the goal of controlling them. However relatively little is known about the its influence on the DLI [9]. Dursi [7] addressed the magnetic DLI, with treating normal and tangential external magnetic field separately, but has gone untouched the coexistent case of the both fields. The latter half of this paper is devoted to handling simultaneous application of the both fields, that is, the oblique external magnetic field. This case exhibits a marked contrast with the cases of a single component, in the sense that only the genuinely oblique magnetic field is able to admit a discontinuity of tangential velocity. For a neutral fluid, the non-zero mass flux is in no way compatible with the tangential-velocity discontinuity, and hence, an oblique magnetic field may drastically alter the DLI. The coexistence of the DLI and the KHI is of our primary concern, and we shall shoe that this is indeed the case.

The detail of derivation of the jump conditions across the flame front is not often described in the literature [7]. We begin, in section 2, with it, following the method of refs [1, 11]. As a reward, a generalization is achieved to incorporate the disparity of the magnetic permeability and to correct the Markstein effect. With these jump conditions as a basis, we revisit, in section 3, the effect of the tangential magnetic field on the DLI. We include the gravity, the surface tension and the Markstein effects, and look into the effect of the disparity of the magnetic permeability, which are missing in [7]. Section 4 focuses on the effect of the obliques magnetic field. As anticipated above, we find a possible emergence of the KHI to compete with the stabilizing action of the magnetic field. We close, in section 5, with a summary and a list of remaining problems.

2 Basic equations and jump conditions

The governing equations of the magnetohydrodynamics of an inviscid, incompressible and perfectly conducting fluid are

$$\frac{\partial \vec{U}}{\partial t} + (\vec{U}\cdot\nabla)\vec{U} - \frac{1}{\rho\mu}(\vec{B}\cdot\nabla)\vec{B} + \nabla\left(\frac{\vec{B}^2}{2\rho\mu}\right) = -\frac{1}{\rho}\nabla P + \vec{g}\frac{\delta\rho}{\rho}, \tag{1}$$

$$\frac{\partial \vec{B}}{\partial t} - \nabla\times(\vec{U}\times\vec{B}) = 0, \tag{2}$$

$$\nabla\cdot\vec{U} = 0, \tag{3}$$

$$\nabla\cdot\vec{B} = 0, \tag{4}$$

where $\vec{U}$ is the velocity, $\vec{B}$ is the magnetic field, ρ is the density, p is the pressure, μ is the magnetic permeability and $\vec{g} = (0,0,-g)$ is gravity acceleration directed in the negative z-axis. For sake of simplicity, we employ the Boussinesq approximation to treat the buoyancy effect.

We put the xy-plane parallel to the unperturbed planer flame front and the z-axis is perpendicular to it with the front lying on $z = 0$. In the sequel, we derive the boundary conditions, or the jump conditions, across the flame front, from the unburned to the burned sides, by utilizing the Heaviside step function $H(\theta)$ defined by

$$H(\theta) = \begin{cases} 1 & (\theta > 0) \\ 0 & (\theta < 0) \end{cases}, \tag{5}$$

[1, 10, 11]. This function is used to express the discontinuity of the basic flow outside a flame front. The Dirac delta function $\delta(\theta)$ appears as the derivative of the Heaviside step function.

$$\delta(\theta) = \frac{d}{d\theta} H(\theta).$$

The position of the perturbed flame front is set to be $z = \zeta(x,y,t)$. In deriving the jump conditions across the flame front, it is useful to introduce $\theta = \zeta(x,y,t) - z$ with the flame located at $\theta = 0$. The unit normal vector to the flame front is expressed as

$$\vec{n} = \nabla\theta/|\nabla\theta| \approx (\nabla\zeta, -1). \tag{6}$$

The normal component of the velocity of a flame front is

$$\vec{u}_f \cdot \vec{n} = -\frac{\partial\zeta}{\partial t}, \tag{7}$$

and $\dot{\theta} = \partial\theta/\partial t = \partial\zeta/\partial t$. We should keep in mind that $\theta < 0$ and $\theta > 0$ represent the burned and unburned regions respectively.

With this setting, the density field $\rho = \rho(\vec{x},t)$, for example, is expressed as

$$\rho(\vec{x},t) = \rho_u(\vec{x},t)H(\theta) + \rho_b(\vec{x},t)H(-\theta). \tag{8}$$

Here the subscripts b and u denote the quantities on the burned and the unburned sides, respectively. Substituting (8) and the corresponding representations of the other hydrodynamic and thermodynamic variables into the MHD equations (2)-(4), each of equations is divided into three independent parts, identified respectively by $H(\theta)$, $H(-\theta)$ and $\delta(\theta)$. The part including $H(\theta)$ corresponding to the equation on the unburned side, and the one including $H(-\theta)$ corresponding to the equation on the burned side.

The jump conditions across the flame front are gained by picking up the terms including $\delta(\theta)$. We introduce the notation for the jump of any function f across a flame front,

$$[f] = f_b|_{\theta=0_-} - f_u|_{\theta=0_+}.$$

The unit normal vector $\vec{n}$ and the tangential vectors $\vec{t}_1$ and $\vec{t}_2$ on the flame front are given by $\vec{n} \approx (\partial\zeta/\partial x, \partial\zeta/\partial y, -1)$, $\vec{t}_1 \approx (1, 0, \partial\zeta/\partial x)$ and $\vec{t}_2 \approx (0, 1, \partial\zeta/\partial y)$. We denote the mass flux across the flame front by $\vec{q} = \rho(\vec{u} + \dot{\theta}\vec{n}/|\nabla\theta|)$, with $|\nabla\theta| \approx 1$ to be understood. We take the surface tension, with its coefficient σ, into consideration in the jump condition. The surface tension term appears only in the jump condition. With this setting, we write down the jump conditions. To first order in perturbation amplitude, they read

$$[\vec{q}\cdot\vec{n}] = 0, \tag{9}$$

$$[\vec{B}\cdot\vec{n}] = 0, \tag{10}$$

$$[\vec{U}\cdot\vec{t}](\vec{q}\cdot\vec{n}) - (\vec{B}\cdot\vec{n})\left[\frac{\vec{B}\cdot\vec{t}}{\mu}\right] = 0, \tag{11}$$

$$[\vec{U}\cdot\vec{n}](\vec{q}\cdot\vec{n}) = -\left[p + \frac{\vec{B}^2}{2\mu}\right] + \left[\frac{1}{\mu}\right](\vec{B}\cdot\vec{n})^2 + \sigma\left(\frac{\partial^2\zeta}{\partial x^2} + \frac{\partial^2\zeta}{\partial y^2}\right), \tag{12}$$

$$(\vec{q}\cdot\vec{n})\left[\frac{\vec{B}\cdot\vec{t}}{\rho}\right] = (\vec{B}\cdot\vec{n})[\vec{u}\cdot\vec{t}]. \tag{13}$$

These jump conditions (11) and (12) accomplish an extension of the previous ones [18, 7, 10] to include the effect of the difference of the magnetic permeability.

It is worthwhile to recollect Landau's assumption. The flame speed S_f is the speed of the gas incoming to the flame front. Noting that vector $\vec{n}$ is directed to the unburned side, it is given by

$$S_f = \vec{U}_u|_{\theta=0_+}\cdot(-\vec{n}) - \vec{u}_f\cdot(-\vec{n}), \tag{14}$$

where $\vec{u}_f\cdot\vec{n}$ is normal perturbation speed of the flame front. Landau's assumption is interpreted as $S_f = S_L$ [6, 13, 14], though generically the flame front is not flat. This assumption is too restrictive. One of the major efforts to improve the original DLI was to incorporate effect of the flame curvature. It is now established as the Markstein effect [15, 5]. In section 3.4, we look into the Markstein effect in the context of the magnetic DLI in the presence of parallel magnetic field.

3 Magnetic DLI subject to tangential magnetic field

In this section, we derive the growth rate when magnetic field parallel to the front is imposed. We follow closely the approach and notation of Dursi [7].

3.1 Hydromagnetic waves

We consider velocity, magnetic fields and pressure of the form

$$\vec{U} = (u, v, w+W) \qquad (u, v, w \ll W), \tag{15}$$

$$\vec{B} = (b_x + B, b_y, b_z) \qquad (b_x, b_y, b_z \ll B), \tag{16}$$

$$P = P_0 + p \qquad (p \ll P_0), \tag{17}$$

where W, B and P_0 are the values of the basic state, which are taken to be constants within each region. The jump conditions (9) and (13) require jump of the values of W and B across the flame front by

$$[\rho W] = 0, \quad [WB] = 0. \tag{18}$$

These physical quantities may vary rapidly but smoothly inside the flame front [16, 3, 4, 19], but we do not pursue it in this paper.

We take the perturbation of normal form $e^{i\vec{k}\cdot\vec{x}+nt}$ with infinitesimal amplitude. Here the wavevector is defined as $\vec{k} = (k_x, k_y)$ with its magnitude being $k = \sqrt{k_x^2 + k_y^2}$ and n is the growth rate of the wave on the flame front. Here, we exclusively deal with two-dimensional deformation $\vec{k} = (k_x, 0)$

The linearized equations are obtained by substituting (15)-(17) into (1)-(4). We find that a perturbed quantity is expressed by a linear combination of the following modes [7]:

$$\left(C_1 e^{kz} + C_2 e^{-kz} + C_3 e^{-\frac{n+iak_x}{W}z} + C_4 e^{-\frac{n-iak_x}{W}z}\right) e^{i\vec{k}\cdot\vec{x}+nt}, \tag{19}$$

where $a = B/\sqrt{\mu\rho}$ is the the Alfvén speed. It should be born in mind that the Alfvén modes, with amplitude C_3 and C_4, have a distinguishing feature of possessing the vorticity. There is another mode in each region, but this mode turns out to vanish and is irrelevant. We note that the perturbation must be finite. Provided that the real part $\mathrm{Re}[n] > 0$ for instability, the unburned side accepts only the mode with amplitude C_1 and the burned side accepts modes with C_2, C_3 and C_4. The vorticity field introduced on the burned side for a neutral fluid [13, 14] is realized by the Alfvén waves, having amplitude C_3 and C_4, for the MHD.

3.2 Linear perturbations in unburned and burned regions

At the outset, we specify a possible combination of waves for b_{ux} and b_{bx}. By integrating the linearized MHD equations, we obtain the expressions for perturbed quantities as follows [7].

On the unburned side, we have

$$b_{ux} = B_u C_1 e^{kz}, \tag{20}$$

$$b_{yu} = B_u \frac{k_y}{k_x} C_1 e^{kz}, \tag{21}$$

$$b_{uz} = -iB_u \frac{k}{k_x} C_1 e^{kz}, \tag{22}$$

$$u_u = -i\frac{(n+W_u k)}{k_x} C_1 e^{kz}, \tag{23}$$

$$v_u = -i\frac{(n+W_u k)k_y}{k_x^2} C_1 e^{kz}, \tag{24}$$

$$w_u = -\frac{(n+W_u k)}{k}(1+\frac{k_y^2}{k_x^2}) C_1 e^{kz}, \tag{25}$$

$$p_u = \frac{\rho_u (n+W_u k)^2}{k_x^2} C_1 e^{kz}. \tag{26}$$

On the burned side, we have

$$b_{bx} = B_b C_2 e^{-kz} + B_b C_3 e^{-\frac{n+ia_b k_x}{W_b} z} + B_b C_4 e^{-\frac{n-ia_b k_x}{W_b} z}, \tag{27}$$

$$b_{yb} = \frac{k_y}{k_x} B_b C_2 e^{-kz} + B_b C_5 e^{-\frac{n+ia_b k_x}{W_b} z} + B_b C_6 e^{-\frac{n-ia_b k_x}{W_b} z}, \tag{28}$$

$$\begin{aligned} b_{bz} = {} & iB_b \frac{k}{k_x} C_2 e^{-kz} + iW_b B_b \frac{k_x C_3 + k_y C_5}{n+ia_b k_x} e^{-\frac{n+ia_b k_x}{W_b} z} \\ & + iW_b B_b \frac{k_x C_4 + k_y C_6}{n-ia_b k_x} e^{-\frac{n-ia_b k_x}{W_b} z}, \end{aligned} \tag{29}$$

$$u_b = -\frac{i}{k_x}(n-W_b k) C_2 e^{-kz} - a_b C_3 e^{-\frac{n+iak_x}{W_b} z} + a_b C_4 e^{-\frac{n-iak_x}{W_b} z}, \tag{30}$$

$$v_b = -ik_y \frac{n-W_b k}{k_x^2} C_2 e^{-kz} - a_b C_5 e^{-\frac{n+iak_x}{W_b} z} + a_b C_5 e^{-\frac{n-iak_x}{W_b} z}, \tag{31}$$

$$\begin{aligned} w_b = {} & \frac{(n-W_b k)k}{k_x^2} C_2 e^{-kz} - i\frac{W_b (k_x C_3 + k_y C_5)}{n+ia_b k_x} a_b e^{-\frac{n+iak_x}{W_b} z} \\ & + i\frac{W_b (k_x C_4 + k_y C_6)}{n-ia_b k_x} a_b e^{-\frac{n-iak_x}{W_b} z}, \end{aligned} \tag{32}$$

$$p_b = \rho_b \frac{(n-W_b k)^2}{k_x^2} C_2 e^{-kz} - (\rho_b a_b^2) C_3 e^{-\frac{n+iak_x}{W_b} z} - (\rho_b a_b^2) C_4 e^{-\frac{n-iak_x}{W_b} z}. \tag{33}$$

3.3 Jump conditions and dispersion relation

We specialize the jump conditions (9)-(13) to the case in which only magnetic field parallel to the flame front is externally imposed in the unperturbed state. These jump conditions reduce to

$$[b_z - \frac{ik_x}{n} wB] = 0, \tag{34}$$

$$\rho W[u + \frac{ik_x}{n} wW] - (b_z - \frac{ik_x}{n} wB)[\frac{B}{\mu}] = 0, \tag{35}$$

$$\rho W[v + \frac{ik_y}{n} wW] = 0, \tag{36}$$

$$[p + \frac{Bb_x}{\mu}] = \frac{gw}{n}[\rho] + \sigma(\frac{\partial^2 \zeta}{\partial x^2} + \frac{\partial^2 \zeta}{\partial y^2}), \tag{37}$$

$$[Wb_x] = 0, \tag{38}$$

$$[Wb_y] = 0. \tag{39}$$

In (37), we see the the gravity effect entering into in jump condition for the pressure.

In view of (7), Landau's assumption dictates that

$$-w_u + \frac{\partial \zeta}{\partial t} = 0. \tag{40}$$

The jump condition (9) then tells us that

$$-w_b + \frac{\partial \zeta}{\partial t} = 0. \tag{41}$$

We take the advantage of (40), or equivalently (41), to eliminate ζ.

According to the zeroth-order relations in jump conditions

$$\frac{\rho_u}{\rho_b} = \frac{W_b}{W_u} = \frac{B_u}{B_b} = \alpha,$$

we make the following replacement $\rho_b = \rho_u/\alpha, W_b = \alpha W_u$ and $B_b = B_u/\alpha$. We introduce dimensionless variables $\bar{n} = n/kW_u$, the growth rate, $\bar{a}_u = a_u/W_u$, $\bar{\sigma} = \sigma k/\rho_u W_u^2$, $\bar{g} = g/kW_u^2$, $\bar{k}_x = k_x/k$, $\bar{k}_y = k_y/k$ and $\nu = \mu_u/\mu_b$. After some manipulation, we cast the jump conditions into a system of linear equations $\vec{M} \cdot (C_1, C_2, C_3, C_4, C_5, C_6)^T = 0$ with a square matrix $\vec{M}$. For the existence of nontrivial perturbation $(C_1, C_2, C_3, C_4, C_5, C_6) \neq \vec{0}$, the determinant of $\vec{M}$ should be zero, and we arrive at the eigenvalue equation for $\bar{n}$.

$$\begin{aligned} &\left\{\bar{a}_u^2 \bar{k}_x^2 + (\bar{n} - \alpha)^2 \alpha \nu\right\} \left\{\bar{a}_u^2 \bar{k}_x^2 (1 + \bar{n} - 2\alpha + \alpha^2 \nu + \bar{n}\alpha^2 \nu)\right. \\ &\left. + (1 + \bar{n})\alpha\nu \left(\bar{g}(-1 + \alpha) + 2\bar{n}\alpha + \bar{n}^2(1 + \alpha) + \alpha(1 - \alpha + \bar{\sigma})\right)\right\} = 0. \end{aligned} \tag{42}$$

This result extends Dursi's dispersion relation [7] to include the difference of the magnetic permeability as indicated by ν. The magnetic permeability depends on the material and the temperature. As a typical astrophysical combustion, the supernova is considered to be a diamagnetic object ($\nu < 1$).

3.4 Markstein effect

This subsection focuses on the Markstein effect, putting aside the effect of the surface tension ($\sigma = 0$). Markstein [15] amended Landau's assumption phenomenologically by including the effect of the flame-front curvature on the flame speed. As a consequence, Landau's condition is augmented with a term proportional to the front curvature.

$$S_f = -(\vec{U}_u \cdot \vec{n} - \nu \cdot \vec{n}) = S_L(1 - \mathscr{L}\Delta\zeta), \tag{43}$$

where the coefficient $\mathscr{L}$ (> 0) is referred to as the Markstein length.

At the zeroth order, the flame velocity coincides with the laminar flame speed S_L and balances with the basic flow on the unburned side.

$$W_u = S_L. \tag{44}$$

The variation of linear order in (43) incorporates the curvature effect.

$$w_u - \frac{\partial\zeta}{\partial t} = -S_L\mathscr{L}\Delta\zeta. \tag{45}$$

As before, we substitute superposition of the basic flow and perturbations to (34)-(39) and (43). Landau's condition (40) is taken over by (45). For a normal mode $\zeta \sim e^{ik\vec{x}+nt}$, (45) reads

$$w_u = (W_u\mathscr{L}k^2 + n)\zeta, \tag{46}$$

by virtue of $S_L = W_u$,

We restrict our attention to the 2D problem on the xz-plane, and take $k_y = 0$ and $C_5 = C_6 = 0$. With the help of (46), we replace ζ by w_u. Repeating the same procedure, we transform the jump conditions to a system of 4 linear equations $\vec{M} \cdot (C_1, C_2, C_3, C_4)^T = 0$. The condition of vanishing the determinant of matrix $\vec{M}$ yields

$$\begin{aligned}
&\left\{\bar{a}_u^2\bar{k}_x^2 + (\bar{n} - \alpha)^2\alpha\nu\right\}\left\{\bar{a}_u^2\bar{k}_x^2(1 + \bar{n} + 2(-1 + \overline{\mathscr{L}})\alpha + \alpha^2\nu + \bar{n}\alpha^2\nu)\right. \\
&\left. + (1 + \bar{n})\alpha\nu\left(\bar{g}(-1 + \alpha) + 2(1 + \overline{\mathscr{L}})\bar{n}\alpha + \bar{n}^2(1 + \alpha) + \alpha(1 - \alpha + 2\overline{\mathscr{L}}\alpha + \bar{\sigma})\right)\right\} \\
&= 0,
\end{aligned} \tag{47}$$

where $\overline{\mathscr{L}} = \mathscr{L}k$ is the dimensionless Markstein length, or the Markstein number.

Given typical values of the Markstein number $\overline{\mathscr{L}} = 0.1$ and the dimensionless gravity acceleration $\bar{g} = 2$, we draw in Fig. 1 the stability boundary ($\mathrm{Re}[n] = 0$) in the parameter space of $\bar{a}_u = B_u/\sqrt{\rho_u\mu_u}$ and α, for various values of the ratio $\nu = \mu_u/\mu_b$ of the magnetic permeability. To this aim, we resort to the Routh-Hurwitz or the Lienard and Chipart criterion for roots of a polynomial equation [2, 8, 12]. The boundary curves correspond to $\nu = 4, 1, 0.5, 0.3$ from left to right, except that the stability region is splitted into two parts for $\nu = 0.3$ and 0.5. The dark region, the right hand side of the curve, except for $\nu = 0.3$ and 0.5, corresponds to the stable

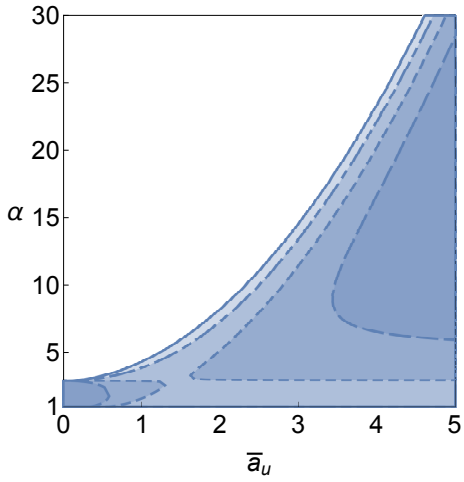

Fig. 1 Dependence on the magnetic-permeability ratio $\nu = \mu_u/\mu_b$ of stability boundary of the magnetic DLI in the plane of the tangential magnetic field $\bar{a}_u = B_u/\sqrt{\rho_u \mu_u}$ and the thermal expansion α ($1 < \alpha < 30$), with the Markstein ($\overline{\mathscr{L}} = 0.1$) and the gravity ($\bar{g} = 2$) effects taken into account. The boundary curves correspond to $\nu = 4, 1, 0.5, 0.3$ from left to right. Colored region (the right hand side of each curve) corresponds to stability region. Notice that stability region is splitted into two regions for $\nu = 0.5$ and 0.3.

parameters, meaning that stronger tangential magnetic field is able to suppress the DLI. For smaller α, the critical value of $\bar{a}_u$ for stability is smaller. The stability region depends sensitively on the magnetic-permeability ratio. The stability region shrinks as ν decreases, implying that the diamagnetic fuel ($\nu < 1$), as is the case of a supernova, enhances the DLI.

We point out that Dursi [7] made an attempt at incorporating the Masrkstein effect into the magnetic DLI. He applied the Markstein condition (45) not only to the unburned side, but also burned side. However, the condition (45) is applicable only to w_u, the burned side.

4 Magnetic DLI subject to oblique magnetic field

We turn to the general case of presence of both the parallel and normal components of external magnetic field, which was not considered in the previous investigation [7]. We reveal that the simultaneous existence of parallel and normal components drastically alters the situation of a single component. Only when the both components are present, discontinuity of the tangential velocity along the flame front is induced, which may cause the Kelvin-Helmholtz instability (KHI). For the sake of simplicity, we disregard the jump of the magnetic permeability across the flame front and take the common value μ_0 of the vacuum for the both sides.

4.1 Jump of basic state

Consider a superposition of the basic state with the unperturbed flame front lying on the plane of $z=0$, imposed by the external magnetic field (B_x, B_z) imposed, and linear perturbation to it. We restrict our attention to the two-dimensional flow in the xz-plane, and express the flow field as

$$\vec{U} = (u+U, w+W) \qquad (|u|, |w| \ll |U|, |W|), \tag{48}$$

$$\vec{B} = (b_x + B_x, b_z + B_z) \qquad (|b_x|, |b_z| \ll |B_x|, |B_z|), \tag{49}$$

$$\tilde{p} = P + p \qquad (|p| \ll |P|). \tag{50}$$

If we set $U=0$ and $B_z=0$, the situation reduces to the case considered in section 3.

We examine the jump conditions (9)-(13) in this general context. Substituting the basic flow field among (48)-(50), these jump conditions become

$$[\rho W] = 0, \tag{51}$$

$$[B_z] = 0, \tag{52}$$

$$[U]\rho W - \frac{B_z}{\mu_0}[B_x] = 0, \tag{53}$$

$$[WB_x] = B_z[U]. \tag{54}$$

The first two conditions give $\alpha W_u = W_b$ and $B_z := B_{uz} = B_{bz}$, by use of the thermal expansion rate $\alpha = \rho_u/\rho_b$. Simultaneous solution of (53) and (54) gives rise to

$$[U] = W_u \frac{a_{ux}}{a_{uz}} \frac{(1-\alpha)a_{uz}^2}{\alpha W_u^2 - a_{uz}^2}, \tag{55}$$

$$B_{bx} = B_{ux} \frac{W_u^2 - a_{uz}^2}{\alpha W_u^2 - a_{uz}^2}, \tag{56}$$

where $a_{ui} = B_{ui}/\sqrt{\rho_u \mu_0}$ $(i = x, z)$ is the Alfvén speed on the unburned side and $a_{bi} = B_{bi}/\sqrt{\rho_b \mu_0}$ the Alfvén speed on the burned side.

It is remarkable that the discontinuity of the tangential velocity U is induced, as opposed to the case of section 3. As is well known, in the absence of the magnetic field, the presence of mass flux penetrating through a discontinuous interface requires continuity of the tangential velocity [14], and hence rules out the possibility of the KHI. The distinguishing feature of the case of oblique magnetic field is emergence of tangential discontinuity $[U](\neq 0)$, which is made possible only by the simultaneous application of B_x and B_z as is seen from (55). It is also noteworthy that the relation between B_{ux} and B_{bx} is different from the case of the parallel magnetic field, in section 3, due to the imposition of $B_z(\neq 0)$.

4.2 Hydromagnetic waves

We send perturbations of the form e^{ikx+nt} and expand the MHD equations (1)-(4) to linear order in the perturbation amplitude.

$$(n+Uik+WD)u-\frac{B_z}{\rho\mu_0}Db_x+\frac{B_z}{\rho\mu_0}ikb_z=-\frac{ik}{\rho}p, \tag{57}$$

$$(n+Uik+WD)w-\frac{B_x}{\rho\mu_0}ikb_z+\frac{B_x}{\rho\mu_0}Db_x=-\frac{1}{\rho}Dp, \tag{58}$$

$$(n+Uik+WD)b_x=(B_xik+B_zD)u, \tag{59}$$

$$(n+Uik+WD)b_z=(B_xik+B_zD)w, \tag{60}$$

$$iku+Dw=0, \tag{61}$$

$$ikb_x+Db_z=0, \tag{62}$$

where we have introduced the differential operator $D=d/dz$.

To gain the z-dependence of perturbed variables, we combine (57)-(62) into a single equation. Applying D to (57) and adding it to $-ik$ times (58), we have

$$(n+Uik+WD)(Du-ikw)-\frac{1}{\rho\mu_0}(B_xik+B_zD)(Db_x+ikb_z)=0. \tag{63}$$

Substituting u from (61) and b_x from (62), we further reduce ik times (63) to

$$(n+Uik+WD)(D^2-k^2)w-\frac{1}{\rho\mu_0}(B_xik+B_zD)(D^2-k^2)b_z=0. \tag{64}$$

Applying (B_xik+B_zD) to (64) to eliminate w, with use of (60), we are eventually left with

$$(D^2-k^2)\left\{(n+Uik+WD)^2-\frac{1}{\rho\mu_0}(B_xik+B_zD)^2\right\}b_z=0. \tag{65}$$

The first factor corresponds to the incompressible limit of the sound wave, and the second factor represents the Alfvén waves for the oblique magnetic field, modified by the Doppler effect. The MHD offers the Alfvén waves as agents of carrying the vorticity with them.

4.3 Linear perturbations in unburned and burned regions

In each region, the perturbation should not diverge in the far region from the flame front, as $z\to-\infty$ on the unburned region and as $z\to\infty$ on the burned side. We seek the instability and suppose that $\mathrm{Re}[n]>0$. We assume $k>0$ without loss of generality.

A possible combination of linear waves, with their z-dependence specified by (65), in each region is given as follows. In the unburned region ($\theta > 0$), the permissible perturbation is, on the condition that $\mathrm{Re}[-n/(W_u - a_{uz})] > 0$,

$$C_1 e^{kz} + C_2 e^{\frac{-n-U_u ik + a_{ux} ik}{W_u - a_{uz}} z}, \tag{66}$$

where C_1 and C_2 are constants. In the burned region ($\theta < 0$), the permissible perturbation is, on the conditions that $\mathrm{Re}[-n/(W_b + a_{bz})] < 0$ and $\mathrm{Re}[-n/(W_b - a_{bz})] < 0$,

$$C_3 e^{-kz} + C_4 e^{\frac{-n-U_b ik - a_{bx} ik}{W_b + a_{bz}} z} + C_5 e^{\frac{-n-U_b ik + a_{bx} ik}{W_b - a_{bz}} z}, \tag{67}$$

where C_3, C_4 and C_5 are constants. The first condition is necessarily fulfilled for $n > 0$. The wave with C_2 is allowable only in the case of $W_u < a_{uz}$ and that of C_5 only in the case $W_b > a_{bz}$. In the marginal case of $W = a_z$ in either the unburned or burned side, the factor $\{(n + Uik + WD)^2 - (a_x ik + a_z D)^2\}$ in (65) degenerates to $(n + Uik - a_x ik)\{n + Uik + a_x ik + (a_z + W)D\}$, and the corresponding wave, with C_2 or C_5, is lost. In such a degenerate case, separate treatment is required [7].

A concrete representation of the perturbation velocity and magnetic field in each region is determined by (57)-(62). For the sake of simplicity, we set $U = 0$ in the unburned side. Given b_{uz}, the other perturbation variables in the unburned side are built so as to satisfy (57)-(62), resulting in

$$b_{uz} = B_z C_1 e^{kz} + B_z C_2 e^{A_2 z}, \tag{68}$$

$$b_{ux} = iB_z C_1 e^{kz} + \frac{i}{k} A_2 B_z C_2 e^{A_2 z}, \tag{69}$$

$$w_u = B_z \frac{n + W_u k}{B_{ux} ik + B_z k} C_1 e^{kz} + a_{uz} C_2 e^{A_2 z}, \tag{70}$$

$$u_u = B_z i \frac{n + W_u k}{B_{ux} ik + B_z k} C_1 e^{kz} + a_{uz} \frac{i}{k} \frac{-n + a_{ux} ik}{W_u - a_{uz}} C_2 e^{A_2 z}, \tag{71}$$

$$p_u = -\frac{\rho_u}{k} \frac{(n + W_u k)^2}{B_{ux} ik + B_z k} B_z C_1 e^{kz} - \rho_u \left\{ a_{uz}^2 + a_{ux} a_{uz} \frac{i}{k} \frac{-n + a_{ux} ik}{W_u - a_{uz}} \right\} C_2 e^{A_2 z}, \tag{72}$$

where

$$A_2 = \frac{-n + a_{ux} ik}{W_u - a_{uz}}. \tag{73}$$

In case $\mathrm{Re}[n] > 0$, $W_u < a_{uz}$ is required for $\mathrm{Re}[A_2] > 0$. Likewise, given b_{bz}, the perturbation variables on the burned side are found to be

$$b_{bz} = B_z C_3 e^{-kz} + B_z C_4 e^{A_4 z} + B_z C_5 e^{A_5 z}, \tag{74}$$

$$b_{bx} = -iB_z C_3 e^{-kz} + \frac{i}{k} A_4 B_z C_4 e^{A_4 z} + \frac{i}{k} A_5 B_z C_5 e^{A_5 z}, \tag{75}$$

$$w_b = \frac{n + U_b ik - kW_b}{B_{bx} ik - B_z k} B_z C_3 e^{-kz} - a_{bz} C_4 e^{A_4 z} + a_{bz} C_5 e^{A_5 z}, \tag{76}$$

$$u_b = -i \frac{n + U_b ik - W_b k}{B_{bx} ik - B_z k} B_z C_3 e^{-kz} - a_{bz} \frac{i}{k} A_4 C_4 e^{A_4 z} + a_{bz} \frac{i}{k} A_5 C_5 e^{A_5 z}, \tag{77}$$

$$\begin{aligned} p_b = & \frac{\rho}{k} \frac{(n + U_b ik - kW_b)^2}{B_x ik - B_z k} B_z C_3 e^{-kz} \\ & - \rho_b \left\{ a_{bz}^2 + a_{bx} a_{bz} \frac{i}{k} A_4 \right\} C_4 e^{A_4 z} - \rho_b \left\{ a_{bz}^2 + a_{bx} a_{bz} \frac{i}{k} A_5 \right\} C_5 e^{A_5 z}, \end{aligned} \tag{78}$$

where

$$A_4 = \frac{-n - U_b ik - a_{bx} ik}{W_b + a_{bz}}, \tag{79}$$

$$A_5 = \frac{-n - U_b ik + a_{bx} ik}{W_b - a_{bz}}. \tag{80}$$

The condition $\mathrm{Re}[A_4] < 0$ is always satisfied. The condition $\mathrm{Re}[A_5] < 0$ requires $W_b > a_{bz}$. Substituting from (55) and (56), the wave numbers A_2, A_4 and A_5 are expressed in terms of dimensionless variables as

$$\frac{A_2}{k} = \frac{-\bar{n} + \bar{a}_{ux} i}{1 - \bar{a}_{uz}}, \tag{81}$$

$$\frac{A_4}{k} = \left(-\bar{n} - \gamma i \frac{(1-\alpha)\bar{a}_{uz}^2}{\alpha - \bar{a}_{uz}^2} - \sqrt{\alpha} \bar{a}_{ux} i \frac{1 - \bar{a}_{uz}^2}{\alpha - \bar{a}_{uz}^2} \right) \Big/ (\alpha + \sqrt{\alpha} \bar{a}_{uz}), \tag{82}$$

$$\frac{A_5}{k} = \left(-\bar{n} - \gamma i \frac{(1-\alpha)\bar{a}_{uz}^2}{\alpha - \bar{a}_{uz}^2} + \sqrt{\alpha} \bar{a}_{ux} i \frac{1 - \bar{a}_{uz}^2}{\alpha - \bar{a}_{uz}^2} \right) \Big/ (\alpha - \sqrt{\alpha} \bar{a}_{uz}), \tag{83}$$

where $\bar{n} = n/kW_u$ is the dimensionless growth rate, $\bar{a}_{iu} = a_{iu}/W_u$ the dimensionless Alfvén speed and we have introduced $\gamma = B_{ux}/B_z$, the measure for the angle of the magnetic field from the normal on the unburned side.

4.4 Jump of perturbation fields

We are in a stage to substitute the solution of each region, written out in section 4.3, into the jump conditions (9)-(13) to connect them at the flame front. These jump conditions are no other than the conservation laws of the mass, the momentum and the magnetic flux and the induction equation in a region, of infinitesimal thickness, centered on the flame front [1, 11]. To spotlight the influence of the oblique external magnetic field, we employ Landau's assumption (40).

$$w_u - \frac{\partial \zeta}{\partial t} = 0, \tag{84}$$

and we ignore the gravity force and the surface tension. Recall that the basic state is constructed so as to comply with the jump conditions (51)-(54) to leading order. The remaining task is to satisfy the conditions to first order in perturbation amplitude.

The jump conditions (9)-(13) linearized for perturbed quantities become

$$U_b \frac{\partial \zeta}{\partial x} - w_b + \frac{\partial \zeta}{\partial t} = 0, \tag{85}$$

$$\left[B_x \frac{\partial \zeta}{\partial x} - b_z \right] = 0, \tag{86}$$

$$\rho_u W_u \left[u + W \frac{\partial \zeta}{\partial x} \right] - \frac{B_z}{\mu_0}[b_x] + \left(B_{ux} \frac{\partial \zeta}{\partial x} - b_{uz} \right) \frac{1}{\mu_0}[B_x] = 0, \tag{87}$$

$$\left[p + \frac{B_x b_x + b_z B_z}{\mu_0} \right] = 0, \tag{88}$$

$$[W b_x] - B_z[u] + \left(B_{ux} \frac{\partial \zeta}{\partial x} - b_{uz} \right)[U] = 0. \tag{89}$$

The quantities on both sides of the flame front $z = \zeta$ is evaluated at $z = \pm 0$, because the difference of the values at $z = \pm\zeta$ and those at $z = \pm 0$ add only second-order corrections.

After substituting the solution (68)-(72) and (74)-(78) into (85)-(89) and eliminating ζ by use of (84), we obtain a system of linear algebraic equations $\vec{M} \cdot (C_1, C_2, C_3, C_4, C_5)^T = \vec{0}$. We notice, by an analysis of the 5×5 matrix $\vec{M}$, that, without specifying $\bar{n}$, the rank of of $\vec{M}$ is four and that one of (85), (86) are (89) may be discarded. Retaining (86)-(89), we are left with 4 equations for 5 constants C_1, C_2, C_3, C_4 and C_5, amplitude of the waves. A separate treatment is needed, depending on whether W_u (W_b) is larger or smaller than the Alfvén speed a_{uz} (a_{bz}).

4.5 Growth rate

By removing one of the constants C_1, C_2, C_3, C_4 and C_5, on the physical ground, from the system (86)-(89) of linear algebraic equations, we coin 4×4 non-singular matrix $\hat{\vec{M}}$ from $\vec{M}$. The growth rate $\bar{n}$ is determined by requiring $\det \hat{\vec{M}} = 0$. We have to separately deal with four cases specified by $W_u \lessgtr a_{uz}$ and $W_b \lessgtr a_{bz}$ and, in addition, with the marginal cases specified by $W_u = a_{uz}$ or $W_b = a_{bz}$.

With a view to seeing how the KHI enters the DLI, we concentrate on two cases, super-Alfvénic and sub-Alfvénic in the both regions, with the detailed classification of the results left for a future paper. We begin with the both super-Alfvénic case, the case of smaller magnetic field, as a natural extension of the original DLI. It is to be remembered that $a_{bz} = \sqrt{\alpha} a_{uz}$ because of $B_{bz} = B_{uz}$.

4.5.1 Super-Alfvénic flame: $W_u > a_{uz}, W_b > a_{bz}$

The wave with amplitude C_2 diverges as $z \to -\infty$ because $\mathrm{Re}[A_2] < 0$, and we have to set $C_2 = 0$. The situation becomes the same as that of the classical DLI in the sense that the flow in the unburned region becomes irrotational. In the burned region, the vorticity, emerging from the flame front, is carried by the two Alfvén waves with their propagating velocity $W_b \pm a_{bz} (> 0)$. The coupled system (86)-(89) of linear algebraic equations is the matrix equation with 4×5 matrix $\{\vec{m}_1, \vec{m}_2, \vec{m}_3, \vec{m}_4, \vec{m}_5\}$ represented in the form of an array of columnar vectors $\vec{m}_i$ $(i = 1, \cdots, 5)$. When $C_2 = 0$, $\vec{m}_2$ is excluded, and, with $\bar{n}$ being unspecified, we are left with a non-singular square matrix $\hat{\bar{M}} = \{\vec{m}_1, \vec{m}_3, \vec{m}_4, \vec{m}_5\}$. The requirement of $\det \hat{\bar{M}} = 0$ produces a 5th-order polynomial equation for $\bar{n}$.

$$
\begin{aligned}
&\left\{\alpha^3 - 2\alpha^2(\bar{a}_{uz}^2 - i\bar{a}_{uz}\bar{a}_{ux} + \bar{n}) + \alpha(\bar{a}_{uz}^2 - i\bar{a}_{uz}\bar{a}_{ux} + \bar{n})^2 + (\bar{a}_{ux} + i\bar{a}_{uz}\bar{n})\right\} \\
&\times \Big\{(1+\bar{n})[\alpha^3 + (-i\bar{a}_{ux} + \bar{a}_{uz}\bar{n})^2] \\
&\quad + \alpha[2\bar{a}_{ux}^2 - 2i\bar{a}_{uz}\bar{a}_{ux}(-2 + \bar{a}_{uz}^2 - \bar{n})\bar{n} - \bar{n}(2\bar{a}_{uz}^4 + \bar{n} + \bar{n}^2) \\
&\qquad + \bar{a}_{uz}^2(1 + (3 + 2\bar{a}_{ux}^2)\bar{n} + 3\bar{n}^2 + \bar{n}^3)] \\
&\quad + \alpha^2[\bar{a}_{uz}^2(-1 + \bar{n}) + 2i\bar{a}_{uz}\bar{a}_{ux}\bar{n} - (1+\bar{n})(\bar{a}_{ux}^2 + (1+\bar{n})^2)]\Big\} = 0.
\end{aligned} \tag{90}
$$

Fortunately, this 5th-order equation is factorized into second-order and third-order equations, in the same way as the classical DLI. The roots of the second-order equation are both trivial, with vanishing eigenfunctions $(C_1, C_3, C_4, C_5) = \vec{0}$. Thus the eigen-value equation is simplified into the third-order polynomial equation. If we take the limit $\bar{a}_{ux} \to 0$ of (90), we reproduce the result of Dursi [7] for the magnetic DLI subject only to the normal magnetic field,

$$
\begin{aligned}
&\left\{-\alpha^2 - \bar{n}^2 + \alpha(\bar{a}_{uz}^2 + 2\bar{n})\right\} \\
&\times \left\{(1+\bar{n})(\alpha^2 - \bar{n}^2) - \alpha(1 + 3\bar{n} - 2\bar{a}_{uz}^2\bar{n} + 3\bar{n}^2 + \bar{n}^3)\right\} = 0,
\end{aligned} \tag{91}
$$

and if we take the limit $\bar{a}_{uz} \to 0$, we reproduce (42) with $\nu = 1$ and $\bar{g} = \bar{\sigma} = 0$, supporting for (90).

Figure 2 depicts the stability boundary of the magnetic DLI in the $\bar{a}_{uz}\alpha$-plane ($\bar{a}_{uz} < 1$, $1 < \alpha < 30$) for typical values $2, 3, 4$ and 6 of $\bar{a}_{ux}$. For a polynomial equation with complex constants, the Bilharz criterion applies to determine the neutral stability condition $\mathrm{Re}[\bar{n}] = 0$ [2, 8, 12]. The solid and broken lines correspond to the neutral stability curves for $\bar{a}_{ux} = 6, 4, 3, 2$ from above, except for the case of $\bar{a}_{ux} = 2$ where the neutral stability curve consists two lines. The region below the neutral curve gives parameter values for which the magnetic DLI is suppressed. For $\bar{a}_{ux} = 2$, the region between the two lines is the stability region. Given $\bar{a}_{uz}$, the stability range in the thermal expansion α is widened as $\bar{a}_{ux}$ or B_{ux} is increased. In the super-Alfvénic case in two dimensions, the magnetic DLI can be suppressed by imposing larger tangential magnetic field. When we turn off the tangential magnetic

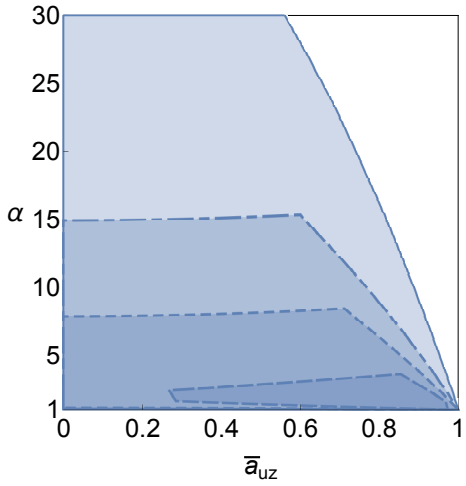

Fig. 2 Variation of stability boundary of the magnetic DLI in the $\bar{a}_{uz}\alpha$-plane ($1 < \alpha < 30$), with obliqueness of the external magnetic field, for the super-Alfvénic flame ($\bar{a}_{uz} = a_{uz}/W_u < 1$). The solid and broken lines correspond to the neutral stability curves for $\bar{a}_{ux} = 6, 4, 3, 2$ from above, except for the case of $\bar{a}_{ux} = 2$ where the neutral curve consists of two lines. The region below the neutral stability curve (the dark side) gives parameter values for which the magnetic DLI is suppressed. The stability region disappears for $\bar{a}_{ux} = 0$.

field ($\bar{a}_{ux} = 0$), the stability region disappears, a result being acceptable as a natural continuation of the DLI for a neutral fluid.

4.5.2 Sub-Alfvénic flame: $W_u < a_{uz}, W_b < a_{bz}$

The effect of the external magnetic field will clearly show up by increasing $B_{uz} = B_{bz}$ so that the Alfvén speed goes beyond the flow speed in each region: $a_{uz} > W_u$ and $a_{bz} > W_b$. In this case, $\mathrm{Re}[A_2] > 0$, and the Alfvén wave with amplitude C_2 is permitted, but, because of $\mathrm{Re}[A_5] > 0$, the Alfvén wave with amplitude C_5 is prohibited. We have to take $C_5 = 0$, while keeping C_2. With this, we reduce the connecting conditions across the flame front to the Matrix equation with non-singular matrix $\hat{\vec{M}} = \{\vec{m}_1, \vec{m}_2, \vec{m}_3, \vec{m}_4\}$. The Alfvén waves traveling away from the flame front are incorporated in both the unburned and burned regions. The vorticity baroclinically created in the flame front is carried, by these Alfvén waves, to both $z \to -\infty$ and $z \to \infty$.

Enforcement of $\det \hat{\vec{M}} = 0$ yields the dispersion relation determining the growth rate $\bar{n}$. As in the super-Alfvénic case, the resulting relation takes the form of 5th-order polynomial equation in $\bar{n}$, which is factorized into a second-order and a third-order polynomial equations. The two roots of the first factor

$$(\bar{n} + 1 - \bar{a}_{uz} - i\bar{a}_{ux}) \left\{ \alpha\sqrt{\alpha} - \sqrt{\alpha}(\bar{a}_{uz}^2 - i\bar{a}_{uz}\bar{a}_{ux} + \bar{n}) - i\bar{a}_{ux} + \bar{a}_{uz}\bar{n} \right\},$$

turn out to be trivial. As a consequence, we have only to solve the third-order polynomial equation. Compared with the the super-Alfvénic case, this equation is lengthy. Below we write down the coefficients of the same power of $\bar{n}$ order by order. The coefficient of $\bar{n}^3$ is

$$(1+\alpha)(\sqrt{\alpha}-\bar{a}_{uz})^2(\sqrt{\alpha}+\bar{a}_{uz}),$$

with no imaginary part. The real part of the coefficient of $\bar{n}^2$ is

$$-(1+\sqrt{\alpha})\sqrt{\alpha}(\sqrt{\alpha}-\bar{a}_{uz})\left\{\alpha^{3/2}-\alpha-2\alpha\bar{a}_{uz}+(1-\sqrt{\alpha})\bar{a}_{uz}^2+2\bar{a}_{uz}^3\right\},$$

and its imaginary part is

$$(1-\sqrt{\alpha})(\sqrt{\alpha}-\bar{a}_{uz})\left\{\alpha^{3/2}+(3+\alpha)\bar{a}_{uz}+\sqrt{\alpha}(1+2\bar{a}_{uz})\right\}\bar{a}_{ux}.$$

The real part of the coefficient of $\bar{n}$ is

$$\begin{aligned}&\alpha^{7/2}-\alpha^3(4+3\bar{a}_{uz})-3\bar{a}_{uz}\bar{a}_{ux}^2+\sqrt{\alpha}(1+2\bar{a}_{uz})\bar{a}_{ux}^2+\alpha^2\bar{a}_{uz}(-1+2\bar{a}_{uz}+\bar{a}_{uz}^2-\bar{a}_{ux}^2)\\&+\alpha^{5/2}(1+6\bar{a}_{uz}+3\bar{a}_{uz}^2+\bar{a}_{ux}^2)-\alpha^{3/2}\bar{a}_{uz}\left\{\bar{a}_{uz}(1+2\bar{a}_{ux}^2)+6\bar{a}_{uz}^2+4\bar{a}_{uz}^3+2\bar{a}_{ux}^2\right\}\\&+\alpha\left\{2\bar{a}_{uz}^4+2\bar{a}_{uz}^5+\bar{a}_{uz}^3(1+2\bar{a}_{ux}^2)+2\bar{a}_{uz}\bar{a}_{ux}^2\right\},\end{aligned}$$

and its imaginary part is

$$-2(1+\sqrt{\alpha})\sqrt{\alpha}\left\{\alpha^{3/2}+\alpha\bar{a}_{uz}^2+\bar{a}_{uz}^2(1+2\bar{a}_{uz})-\sqrt{\alpha}\bar{a}_{uz}(1+3\bar{a}_{uz}+\bar{a}_{uz}^2)\right\}\bar{a}_{ux}.$$

Finally, the real part of the coefficient of $\bar{n}^0$ is

$$(\sqrt{\alpha}-1)(\sqrt{\alpha}+\alpha)(\sqrt{\alpha}-\bar{a}_{uz})\left\{\alpha^2-\alpha(\bar{a}_{uz}^2+\bar{a}_{ux}^2)-(1+2\bar{a}_{uz})\bar{a}_{ux}^2\right\},$$

and its imaginary part is

$$\begin{aligned}&(\sqrt{\alpha}-1)\bar{a}_{ux}\left\{\alpha^3+2\alpha^{5/2}(1+\bar{a}_{uz})-2\alpha^{3/2}\bar{a}_{uz}(1+\bar{a}_{uz})-\bar{a}_{ux}^2\right.\\&\left.+\alpha^2(1-2\bar{a}_{uz}-5\bar{a}_{uz}^2-\bar{a}_{ux}^2)+\alpha\bar{a}_{uz}^2(1+2\bar{a}_{uz}+2\bar{a}_{uz}^2+2\bar{a}_{ux}^2)\right\}.\end{aligned}$$

Figure 3 depicts the stability boundary of the magnetic DLI in the $\bar{a}_{uz}\alpha$-plane ($\bar{a}_{uz}>1$, $1<\alpha<30$) for typical values $2,4$ and 6 of $\bar{a}_{ux}$. The solid line draws $\bar{a}_{uz}=\sqrt{\alpha}$. This line coincides with the critical line $\bar{a}_{ux}=1$, the left-hand side of which is the trans-Alfvénic regime with $W_u<a_{uz}, W_b>a_{bz}$ and the left-hand side of which is the sub-Alfvénic regime, and happens to give the neutral stability curve for all values of $\bar{a}_{ux}(>1)$. The broken lines draw the neutral stability curves for $\bar{a}_{ux}=2,4$ and 6 from inside. The region bounded by the solid line and the broken gives parameter values for which the magnetic DLI is suppressed. This is the region complementary to the banana-shaped region encircled by the dashed line, on the right-hand side of the solid line. For $\bar{a}_{ux}=1$, the whole right-hand side is the stability

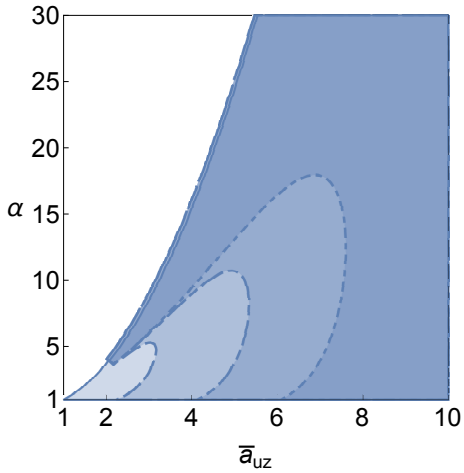

Fig. 3 Variation of stability boundary of the magnetic DLI in the $\bar{a}_{uz}\alpha$-plane ($1 < \alpha < 30$), with obliqueness of the external magnetic field, for the sub-Alfvénic flame ($\bar{a}_{uz} = a_{uz}/W_u > 1$). The solid line $\bar{a}_{uz} = \sqrt{\alpha}$ is the critical line $\bar{a}_{ux} = 1$ dividing the trans-Alfvénic regime (left) from the sub-Alfvénic regime (right) and gives the neutral stability curve for all values of $\bar{a}_{ux}(> 1)$, and the broken lines enclosing banana-shaped regions, with their vertices located at $(\bar{a}_{uz}, \alpha) = (1, 1)$, correspond to the neutral stability curves for $\bar{a}_{ux} = 2, 4, 6$ from inside. The stability parameters lie in the exterior to the banana-shaped region on the right hand side of the solid line. For $\bar{a}_{ux} = 1$, the whole region on the right-hand side of the solid line corresponds to the stability region.

region. The stability region shrinks as $\bar{a}_{ux}$ is increased. Comparing Figs. 2 and 3, the stability boundary exhibits opposite behavior near $(\bar{a}_{uz}, \alpha) = (1, 1)$. In the super-Alfvénic case (Fig. 2), given a moderate value of α, $\alpha = 3$ say, smaller values of $\bar{a}_{uz}(< 1)$ is required for stability, with its critical value larger for a larger value of $\bar{a}_{ux}$. The predominance of B_{ux} over B_{uz} is vital to stability, and the stability region expands as $\bar{a}_{ux}$ is increased. By contrast, in the sub-Alfvénic case (Fig. 3), for $\alpha = 3$, larger values of $\bar{a}_{uz}(> 1)$ is required for stability, with its critical value larger for a larger value of $\bar{a}_{ux}$.

The banana-shaped instability region is a peculiar feature intrinsic to the case of large imposed magnetic field. Given the value of $\bar{a}_{ux}$, it emanates from $(\bar{a}_{uz}, \alpha) = (\bar{a}_{ux}, 1)$. Figure 3 admits an interpretation that, for a moderate value of α, a distinct species of instability with $\bar{a}_{uz} \approx \bar{a}_{ux}$ parasitizes in the stability region of the DLI. Requisite for this instability is simultaneous application of $B_{ux}(\neq 0)$ and $B_{uz}(\neq 0)$, namely, of an oblique external magnetic field, a result drastically different from the case of the tangential magnetic field alone as discussed in section 3 (see also [7]). As emphasized in section 4.1, the tangential velocity discontinuity $[U]$ is induced only in the simultaneous presence of B_{ux} and B_{uz}. It is probable that this instability has an origin of the KHI. A scrutiny of the eigenfunction is required for convincing this. By increasing $\bar{a}_{uz}$ beyond the critical value depending on $\bar{a}_{uz}$, this instability disappears.

The tans-Alfvénic regime ($W_u < a_{uz}, W_b > a_{bz}$), located on the left-handed side of the solid line in Fig. 3, poses a difficult problem of shortage of the jump conditions [7]. As is readily seen from (66) and (67), all the three Alfvén waves with coefficients C_2, C_4 and C_5 are excitable, yet the number of the jump conditions (85)-(89) at the flame front remains the same. Dursi [7] somehow identified an unstable mode over the whole tras-Alfvénic regime, and we rely on this result.

5 Conclusion

In general, the magnetic field is expected to be an agent for stabilizing the instability of an interface, across which the density and/or the velocity are discontinuous (*cf.* [10, 17]). We have explored the influence of the external magnetic field on the Darrieus-Landau instability of a front of a premixed flame, a less investigated problem. Dursi [7] made a pioneering theoretical work on this problem. We have revisited this and have extended to include the effect of the surface tension and of the difference of the magnetic permeability between the unburned and burned gases. Furthermore, we have tackled the case of the oblique magnetic field, a problem left untouched.

To extend the analysis of [7], we have derived the jump conditions from the first principle of the magnetohydrodynamics following [1, 11], whereby we have incorporated the effect of the magnetic permeability disparity, in addition to the surface tension. Section 3 considered the situation in which only the tangential magnetic field is externally imposed. In section 3.4, we have disclosed that the DLI is enhanced for a diamagnetic fuel. For improving Landau's assumption, we have reconsidered the Markstein effect, and have corrected the previous result [7]. The analysis described in section 3 is limited to two dimensions and it is shown that sufficient strong tangential magnetic field is able to subside down the magnetic DLI. We have also carried out the analysis of three-dimensional stability, that is, the stability of a flat flame to disturbances with wavenumber $\vec{k} = (k_x, k_y)$. We can verify that the stabilizing effect of tangential magnetic field $\vec{B}$ is completely lost when it is orthogonal to the wavenumber: $\vec{B} \cdot \vec{k} = 0$.

In section 4, we have dealt with the oblique external magnetic field, the simultaneous application of both the normal and the tangential magnetic field. Only by the existence of the both fields, the discontinuity of the tangential velocity is induced, an unusual situation when the basic flow penetrates the interface. The presence of the tangential-velocity discontinuity offers the situation where the KHI coexists with the DLI. In section 4.5.2, we have captured this symptom for sufficiently strong magnetic field that the Alfvén speed is faster than that of the basic normal flow on the both sides.

This paper has treated only the limited cases, and a substantial effort will be required to grasp an overall perspective of the magnetic field effect. A separate treatment is necessary for the tras-Alfvénic flame, as touched upon at the end of section 4.5.2, and for the marginal cases where the Alfvén speed coincides with the normal-

flow speed in the unburned and the burned regions. Dependence of the magnetic DLI on the effect of the gravity force, the surface tension and the Markstein effect is left for a future study. For astrophysical phenomena as exemplified by supernova explosions [9], the compressibility effect may be called into play. The Markstein effect corrected by the compressibility effect [19] is worth testing.

Acknowledgements We are grateful to Snezhana Abarzhi, Alexander Klimenko, Kaname Matsue, Saleh Tanveer and Keigo Wada for helpful advices and invaluable comments. Y.F. was supported by a Grant-in-Aid for Scientific Research from the Japan Society for the Promotion of Science (grant no.19K03672).

References

1. Abarzhi, S.I., Fukumoto, Y., Kadanoff, L.P.: Stability of a hydrodynamic discontinuity. Phys. Scr. **90**, 018002 (2015)
2. Bilharz, H.: Bemerkung zu einem Satze von Hurwitz. Z. Angew. Math. Mech. **24**, 77-82 (1944)
3. Class, A.G., Matkowsky, B.J., Klimenko, A.Y.: A unified model of flames as gasdynamic discontinuities. J. Fluid Mech. **491**, 11-49 (2003)
4. Class, A.G., Matkowsky, B.J., Klimenko, A.Y.: Stability of planar flames as gasdynamic discontinuities. J. Fluid Mech. **491**, 51-63 (2003).
5. Clavin, P., Searby, G.: Combustion Waves and Fronts in Flows. Cambridge University Press (2016)
6. Darrieus, G.: unpublished works presented at La Technique Moderne (1938)
7. Dursi, L.J.: The linear instability of astrophysical flames in magnetic fields. Astrophys. J. **606**, 1039-1056 (2004)
8. Frank, E.: On the real parts of the zeros of complex polynomials and applications to continued fraction expansions of analytic functions. Trans. Amer. Math. Soc. **62**, 272-283 (1947)
9. Hillebrandt, W., Niemeyer, J.C.: Type IA supernova explosion models. Ann. Rev. Astron. Astrophys. **38**, 191-230 (2000)
10. Hosking, R.J., Dewar, R.L.: Fundamental Fluid Mechanics and Magnetohydrodynamics. Springer Verlag (2016)
11. Ilyin, D.V., Fukumoto, Y., Goddard III, W.A., Abarzhi, S.I.: Analysis of dynamics, stability, and flow fields'structure of an accelerated hydrodynamic discontinuity with interfacial mass flux by a general matrix method. Phys. Plasmas **25**, 112105 (2018)
12. Kirillov, O.N.: Nonconservative Stability Problems of Modern Physics. Walter de Gruyter GmbH, Berlin/Boston (2013)
13. Landau, L.D.: On the theory of slow combustion. Acta Phys. (USSR) **19**, 77-85 (1944)
14. Landau, L.D., Lifshitz, E.M.: Fluid Mechanics: Course of Theoretical Physics Vol. 6, 2nd edn., p. 488 Butterworth-Heinemann (1987)
15. Markstein, G.H.: Experimental and theoretical studies of flame-front stability. J. Aero. Sci. **18**, 199–209 (1951)
16. Matalon, M., Matkowsky, B.J.: Flames as gasdynamic discontinuities. J. Fluid Mech. **124**, 239-259 (1982)
17. Matsuoka, C., Nishihara, K., Sano, T.: Nonlinear interfacial motion in magnetohydrodynamic flows High Energy Density Phys. **31**, 19-23 (2019)
18. Shu, F.H.: Gas Dynamics, Mill Valley: University Science Books (1992)
19. Wada. K., Fukumoto, Y.: Compressibility effect on Markstein number in long-wavelength approximation. 2019 Matrix annals., to appear (2020)